Analysis of Time Series Imaging Approaches for the Application of Fault Classification of Marine Systems

Christian Velasco-Gallego

Department of Naval Architecture, Ocean and Marine Engineering, University of Strathclyde, United Kingdom Department, University/Organization, Country. E-mail: christian.velasco@strath.ac.uk

Iraklis Lazakis

Department of Naval Architecture, Ocean and Marine Engineering, University of Strathclyde, United Kingdom Department, University/Organization, Country. E-mail: iraklis.lazakis@strath.ac.uk

Artificial Intelligence (AI) can enable better coordination between ships by enhancing decision-making processes through the optimisation of marine vessels' communication technologies and the gathering of information via Internet of Ships (IoS). Although some efforts have been made to detect faults and malfunctions that can occur in marine systems, there is a lack of analysis and formalisation of fault identification (a.k.a. fault classification) approaches; the aim of which is to provide a comprehensive description of any considered fault type and its respective nature. To contribute to this unexplored field within the shipping sector, an analysis of a total of seven time series imaging approaches (Gramian Summation Angular Field (GASF), Gramian Difference Angular Field (GADF), Markov Transition Field (MTF), Markov Transition Matrix (MTM), Recurrence Plot (RP), compound of GASF-GADF-MTF, and compound of GASF-GADF-MTF-MTM-RP), is performed, as these approaches have demonstrated their ability to identify fault patterns that can not be perceived when considering the original time series data. The resulting images are presented as input in a Convolutional Neural Network (CNN) for the performance of the classification task. As part of this analysis, a case study on the turbocharger exhaust gas outlet temperature parameter of a bulk carrier's main engine is also introduced. Promising results are obtained when the distinct time series imaging approaches are combined, as the compound GASF-GADF-MTF-MTM-RP achieved the maximum accuracy for the analysed case study. Such results evidence the need of exploiting the field of time series imaging for the identification of faults.

Keywords: Smart maintenance, fault classification, time series imaging, Gramian Angular Field, first-order Markov chain, recurrence plot

1. Introduction

1,217 marine casualties and incidents were reported in 2020 according to MAIB (2020), which is an increase of 127 marine casualties and incidents with regard to 2019. If the costs associated with the marine accidents occurred between January 2012 and September 2019 are also considered, £5.1 billion out of £7.2 billion (+70%) could have been prevented by considering automated mooring systems, on-board technology, autonomous vessels, and automated cargo handling (London Economics et al. 2021). Consequently, a need for innovation and technological investment is imperative required within the shipping sector.

If special attention is given to the consideration of intelligent technologies for the provision of smart maintenance within the maritime sector, it can be perceived that there is not yet a clear technology for such a matter. An aspect that is not aligned with the identified potential of AI applications within the shipping sector to perform the most efficient and economical maintenance (Department for Transport, 2019). Thus, the modernisation of the current O&M activities, which basically rely on either reactive or preventive maintenance (Han et al., 2021), is of preeminent importance within the sector.

To contribute to the enhancement of such practices, an analysis of time series imaging approaches for fault classification of marine systems is proposed. Such a contribution arises from the limited amount of research identified by the authors related to fault classification of marine systems and the importance of this task in a holistic Maintenance Analytics (MA) framework. For instance, most of the studies rely on the analysis of Support Vector Machines (SVMs) (e.g., Cai et al. (2017), Hou et al. (2020), and Tan et al. (2020)). Also, although some other studies have given consideration to the implementation of Deep Learning (DL) methodologies (e.g., Wang et al. (2020), and Senemmar and Zhang (2021)), none of them analysed the utilisation of computer vision techniques for fault classification of marine systems. Accordingly, a total of seven time series imaging approaches are analysed in this study: 1) Gramian Summation Angular Field (GASF), 2) Gramian Difference Angular Field (GADF), 3) Markov Transition Field (MTF), 4) Markov Transition Matrix (MTM), 5) Recurrence Plot (RP), 6) compound of GASF-GADF-MTF, and 7) compound of GASF-GADF-MTF-MTM-RP are. As part of the fault classification framework, the resulting images are presented as input of a Convolutional Neural Network (CNN) for the performance of the classification task.

The remaining paragraphs are structured as follows. Section 2 presents the literature review of studies in which either fault classification methods within the shipping sector or time series imaging approaches for fault classification are introduced. Section 3 introduces the methodology defined for the performance of this analysis. The case study utilised for this analysis is defined in section 4, in which both the results and the future work are also presented. Finally, the conclusions are outlined in section 5.

2. Literature Review

In total, six studies regarding fault classification of marine systems have been identified from the Scopus database. Four of the six identified studies considered a version of SVM for performing the fault classification task. The remaining two studies applied DL approaches, such as LSTM or BPNN. These DL techniques were either deep neural networks or recurrent neural networks. Thus, the consideration of DL techniques for Computer Vision (CV) for fault classification has not been considered within the shipping sector to the best of the authors' knowledge.

If the literature review is expanded to fault classification in general, thus not considering the application sector, various studies regarding time series imaging can be perceived. Although diverse studies were identified, only two distinct approaches were applied: 1) GAF, and 2) FSFSSII. Thus, there is a need for exploring new methods for image representation from time series, due to their promising results in fault classification and forecasting (Zio, 2022). Accordingly, the contributions of this paper are presented hereunder.

- The analysis of a total of 5 distinct time series imaging approaches: 1) GASF, 2) GADF, 3) MTF, 4) MTM, and 5) RP. Two additional approaches were obtained from the combination of the preceding five approaches in order to assess whether the classification performance is enhanced: 1) GASF-GADF-MTF, and 2) GASF-GADF-MTF-MTM-RP. The compound GASF-GADF-MTF is considered due to the promising results obtained in Wang and Oates (2015).
- The consideration of a computer vision deep learning technique for performing the classification task. For this study, the widely known CNN is applied as the image classifier, as this has not been applied for fault classification within the shipping industry to the best of the authors' knowledge.

3. Methodology

Having explored the current gaps that the shipping sector is currently experiencing regarding the fault classification of marine systems, the proposed methodology for this study is graphically represented in Fig. 1. As observed in this figure, the methodology is comprised of a total of three distinct steps. The first step refers to the data pre-processing step, which is usually implemented when considering data-driven methodologies due to the characteristic of the raw dataset. The second step refers to the encoding of the original time series into images. In this step the 7 distinct time series imaging approaches are considered. The third and final step refers to the fault classifier, which is applied by considering a CNN.

3.1. Data pre-processing

The imputation of missing values, and the identification of operational states are just examples of tasks that need to be performed prior to the implementation of data-driven methodologies when considering sensor data collected from marine systems. The implementation of such data pre-processing tasks is performed as presented in Velasco-Gallego (2020), Velasco-Gallego (2021), and Velasco-Gallego (2022). Furthermore, prior to the encoding of the images, rescaling may be required in advance of the implementation of certain approaches (e.g., GASF, GADF), so that all values of the time series fall in the interval [-1,1] or [0,1].

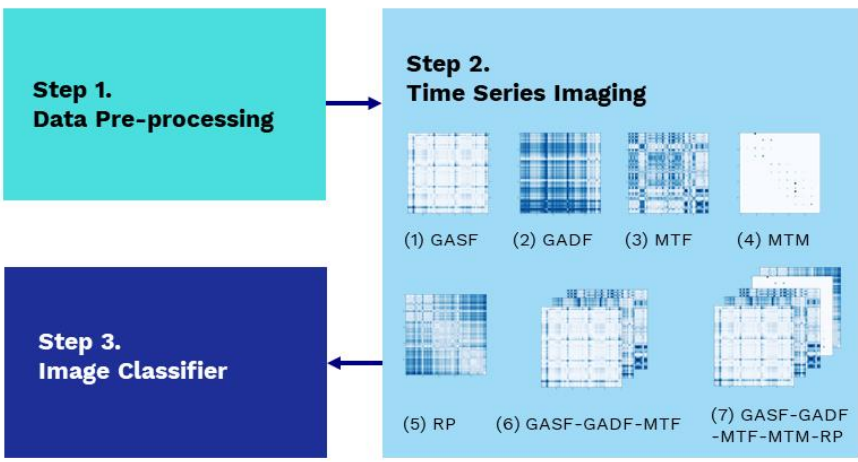

Fig. 1. Graphical representation of the proposed methodology.

3.2. Time series encoding

This step refers to the encoding of time series into images. Accordingly, the following subsections refer to each of the time series imaging approaches being analysed. GASF, GADF, and MTF have been implemented as defined by Wang and Oates (2015). MTM has been applied as introduced by Velasco-Gallego and Lazakis (2022). Lastly, the RP has been defined as indicated in Eckmann et al. (1987).

3.2.1. Gramian Summation Angular Field (GASF)

The first step to be implemented is the representation of the rescaled time series in polar coordinates by encoding each value as the angular cosine and the time stamp as the radius (please see Eq. 1).

$$\begin{cases} \phi = arcos(\tilde{x}_i), -1 \leq \tilde{x}_i \leq 1, \tilde{x}_i \in \tilde{X} \\ r = \dfrac{t_i}{N}, t_i \in \mathbb{N} \end{cases} \tag{1}$$

where t_i is the time stamp and N is a constant factor that aims to regularise the span of the polar coordinate system.

As the polar coordinates have been obtained, the trigonometric sum between each point can be obtained to identify the temporal correlation within the different time intervals. Accordingly, the GASF can be defined as perceived in Eq. 2.

$$GASF = \left[cos(\phi_i + \phi_j)\right] \quad (2)$$

3.2.2. Gramian Difference Angular Field (GADF)

The procedure to obtain the GADF is similar to the one introduced in the preceding section for obtaining GASF. However, GADF is obtained by considering Eq. 3.

$$GADF = \left[sin(\phi_i - \phi_j)\right] \quad (3)$$

3.2.3. Markov Transition Field (MTF)

The MTF is defined as follows:

$$M = \begin{bmatrix} w_{ij|x_1 \in q_i, x_1 \in q_j} & \cdots & w_{ij|x_1 \in q_i, x_n \in q_j} \\ w_{ij|x_2 \in q_i, x_1 \in q_j} & \cdots & w_{ij|x_2 \in q_i, x_n \in q_j} \\ \vdots & \ddots & \vdots \\ w_{ij|x_n \in q_i, x_1 \in q_j} & \cdots & w_{ij|x_n \in q_i, x_n \in q_j} \end{bmatrix} \quad (4)$$

where w_{ij} is given by the frequency with which a point in quantile q_j is followed by a point in quantile q_i.

3.2.4. Markov Transition Matrix (MTM)

Another way of determining the Markov transition matrix is analysed. MTM is determined by following the procedure specified hereunder.

(i) The time series values are clustered in a finite number of states. Such states are determined according to Eq. 2.

$$S_T = \bar{X} \pm ks \quad (5)$$

Where S_T is the state determined, $\bar{X}$ is the mean, and ks is k standard deviations, s, which is added or subtracted until the maximum and the minimum values of the current state are achieved.

(ii) All the possible transition probabilities can be collected in a rxr matrix, where each (i,j) entry P_{ij} is $p(i,j)$,

$$\boldsymbol{P} = \left(P_{ij}\right)_{1 \leq i,j \leq r} \quad (6)$$

$$= \begin{pmatrix} p_{1,1} & p_{1,2} & \cdots & p_{1,r} \\ p_{2,1} & p_{2,2} & \cdots & p_{2,r} \\ \vdots & \vdots & \ddots & \vdots \\ p_{r,1} & p_{r,2} & \cdots & p_{r,r} \end{pmatrix}$$

and that satisfies

$$0 \leq P_{ij} \leq 1, \quad 1 \leq i,j \leq r, \quad (7)$$

$$\sum_{j=1}^{r} P_{ij} = 1, \quad 1 \leq i \leq r. \quad (8)$$

$p(i,j)$ indicates the probability that the previous state i is followed by the current state j.

3.2.5. Recurrence plot (RP)

To obtain the RP, the trajectories need to be determined first. Such trajectories are extracted according to Eq. 9.

$$\vec{x}_i = \left(x_i, x_{i+\tau}, \dots, x_{i+(m-1)\tau}\right), \quad \forall i \in \{1, \dots, n-(m-1)\tau\} \tag{9}$$

where m is the dimension of the trajectories and τ is the time delay. As the trajectories are extracted, the recurrence plot, which is the pairwise distance between trajectories is estimated as shown in Eq. 10.

$$R_{i,j} = \Theta\left(\varepsilon - \left\|\vec{x}_i - \vec{x}_j\right\|\right), \quad \forall i,j \in \{1, \dots, n-(m-1)\tau\} \tag{10}$$

where Θ is the Heaviside function and ε is the threshold.

All the considered time series imaging approaches except for MTM have been implemented by considering the Python library pyts. The MTM approach has been applied by considering the source code of the methodology presented in Velasco-Gallego and Lazakis (2022).

3.2.6. Compound of time series imaging approaches

As part of this analysis, potential compounds between time series imaging approaches are considered. Specifically, a total of two compounds are considered: 1) GASF-GADF-MTF, and 2) GASF-GADF-MTF-MTM-RP. The first compound has been selected based on the promising results obtained in Wang and Oates (2015). The second one has been considered to introduce a compound that presents all the analysed time series imaging methods. Therefore, the input of the image classifier in these instances will present the following shape: (*width of image*, *height of image*, *number of time series imaging approaches included in the compound*).

3.3. Image classifier

To perform the classification task, the CNN is considered, as this DL technique is probably the most widely used when dealing with images. This is a type of feedforward artificial neural network comprised of a feature extraction step and a classification task.

For the first stage, also known as feature extraction, both convolutional layers and pooling layers are considered. Convolutional layers (usually referred to as the main block of the CNN models) consist of a set of filters. These filters convolve with the image and generate a feature map. Specifically, the filter slides over the entire image, and thus the dot product between each element of both the filter and the input can be estimated at every spatial position. A pooling layer is then applied for reducing the dimension of the resulting feature map. Despite the loss of information due to the application of these pooling layers, these can assist by both averting overfitting and reducing the computational cost. This pooling task is implemented by sectioning the input into non-overlapping rectangular subregions so that information from each subregion can be extracted. In this study the max pooling layer is applied.

To perform the classification task, fully connected layers are considered. These layers apply high-level logical operations by considering features from preceding layers. The output of the final layer is a n dimensional vector, which is the total number of classes being considered.

This step is performed by the implementation of the Python libraries Tensorflow and Keras.

4. Results

In order to analyse the performance of each time series imaging approach, a case study is presented on the exhaust gas outlet parameter of one of the cylinders of a main engine of a bulk carrier. In total, approximately 2,000 instances are considered. Such instances have been collected in a 10-minute frequency. The graphical representation of these instances and the descriptive statistics are presented in Fig. 2 and Table 1.

Due to the lack of fault data, abnormal instances need to be simulated. Accordingly, both collective anomalies and degradation patterns, which are two common abnormal scenarios presented when considering parameters collected from marine systems, are generated. The collective anomalies are introduced by considering distinct Gaussian distributions of various mean levels. Such anomalies have been presented in an analogous form as the ones presented in Zhao et al. (2019). By contrast, the degradation patterns have been considered by introducing an exponential model with Brownian motion (please see Li et al., 2021 for a more comprehensive description). Examples of the generated abnormal instances are graphically represented in Figs. 4 and 5. A normal sequence is also presented in Fig. 3 for comparative purposes. Accordingly, a total of three classes are considered for this classification task: 1) normal instances, 2) collective anomalies, and 3) degradation patterns.

The determination of the dimensions of the images have been performed by employing heuristic evaluation. Analogously, the definition of the CNN architecture is also analysed. To adequately compare the performance of each approach, the image dimensions and the CNN architecture are identical for each model. The image dimensions are set to 50x50. The CNN is comprised of two convolutional layers with 192 filters and kernel size of 3x3. A dimension of 2x2 is considered for the pooling operation. With regards to the classification stage, a total of three fully connected layers with 64, 128, and 192 hidden units are considered. The ratio of the training set is set to 0.8 and the test set to 0.2. Analogously, the validation set is also set to 0.2. The epochs and batch size have been selected to be set to 100 and 32, respectively.

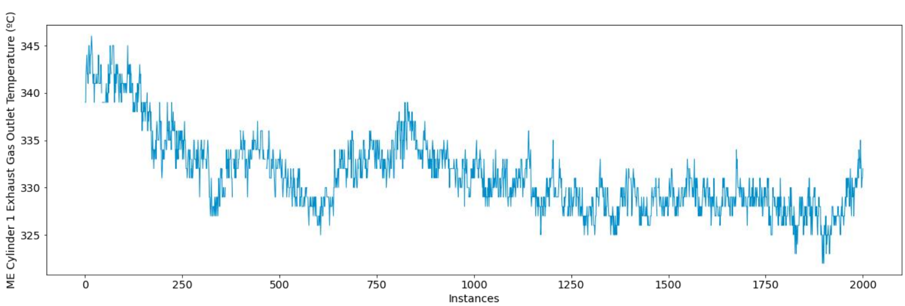

Fig. 2. Graphical representation of the cylinder 1 exhaust gas outlet temperature parameter.

Table 1. Descriptive statistics of the monitored parameter.

	Count	Mean	Std.	Min.	25%	50%	75%	Max.
ME Cylinder 1 Exhaust Gas Outlet Temperature (ºC)	1951	331.31	4.06	322	328	331	333	346

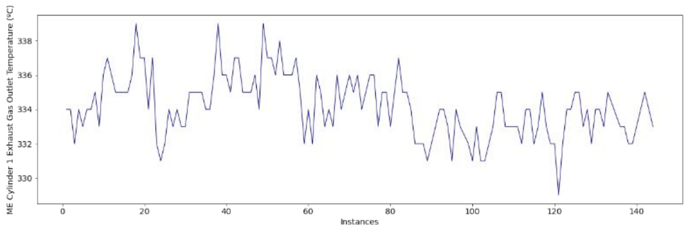

Fig. 3. Example of a normal sequence.

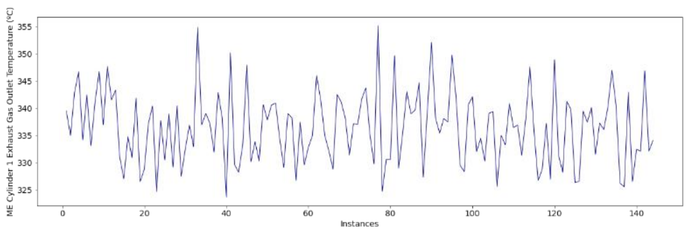

Fig. 4. Example of a sequence with collective anomalies.

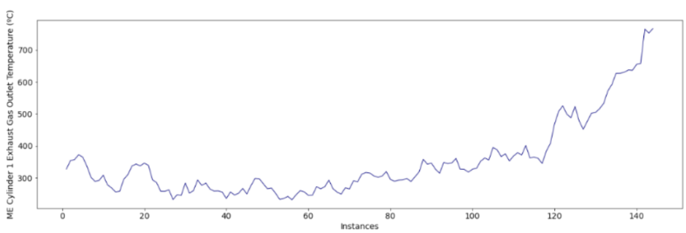

Fig. 5. Example of a sequence with a degradation pattern.

The results of the classification task are introduced in Table 2. The metrics estimated have been selected based on the study presented by Grandini et al. (2020). The combination of all the time series imaging approaches considered presented the most accurate results, leading to the maximum accuracy that can be achieved in a classification task. Although a simple classification task was presented in this study and a decrease in the performance is expected in more complex fault classification tasks that will be conducted in future research, such an aspect demonstrates the potential of time series imaging approaches and the need to perform further research in this field in order to enhance the current practices that the shipping industry is currently applying. The RP and the combination of GASF-GADF-MTF are also leading the ranking, obtaining an accuracy of 99% and 98% respectively. The least accurate results are obtained when considering the GADF, which obtained a maximum accuracy of 75%, that is a decrease of 25% in the accuracy with respects to the most effective model (compound of GASF-GADF-MTF-MTM-RP).

Therefore, as stated precedingly, time series imaging approaches and image classification models are potential fields to exploit to obtain significant enhancements when considering fault classification tasks. To ensure such enhancements, future work guidelines are presented hereunder.

- As presented in the literature review, there is a limited research performed with regards to time series imaging and fault classification. In fact, only two time series imaging approaches have been considered to the best of the authors' knowledge. These are GAF and FSFSSII. Thus, a comprehensive analysis of the approaches presented in other domains and the potential applications of these in the fault classification field is required.

- When performing the heuristic evaluation for the selection of the dimensions of the images, it has been perceived that its selection is of preeminent importance for the adequate performance of the classification task. Thus, a comprehensive analysis of the impact that the dimension of the images has in the performance of the classification task is also needed.
- Only the CNN has been considered as the image classifier. Despite its undeniable performance, other state-of-the-art image classifiers are worth considering.
- The case study presented in this research is based on simulated data due to the lack of fault data. Moreover, only a total of three highly distinctive classes were considered, thus simplifying the classification process. Although such a case study was sufficient to assess the analysed time series imaging approaches, more complex case studies with real-world fault data is needed to exploit the full potential of such methods. Furthermore, only three classes have been considered for this classification task. More classes are expected to be included in the classification task as data accessibility increases.
- A few metrics have been utilised in this study for validation purposes. Further metrics are expected to be included to analyse the obtained results in more detail (e.g., specificity, precision, and confusion matrix).
- Present model explainability for the implemented DL models.
- Assess the utility of employ transfer learning.

Table 2. Classification metric results for the performance of the fault classification task.

Time series approaches	**Accuracy**	**Balanced Accuracy**	**Micro F1**	**Macro F1**	**Weighted F1**	**MCC**	**Kappa**
GASF-GADF-MTF-MTM-RP	1.00	1.00	1.00	1.00	1.00	1.00	1.00
RP	0.99	0.99	0.99	0.99	0.99	0.98	0.98
GASF-GADF-MTF	0.98	0.98	0.98	0.98	0.98	0.97	0.97
MTF	0.94	0.93	0.94	0.94	0.94	0.91	0.90
GASF	0.92	0.94	0.92	0.93	0.92	0.89	0.89
MTM	0.92	0.93	0.92	0.92	0.92	0.89	0.88
GADF	0.75	0.80	0.75	0.76	0.77	0.69	0.64

5. Conclusions

The fault identification, a.k.a. fault classification, is one of the phases considered in the diagnostics analytics module of any MA framework for the identification of the failure modes and their causes. Thus, the relationship between the monitoring data and the fault condition is established. Despite its criticality for the diagnosis of marine systems, it is still an unexplored area within the shipping industry due to current challenges that need to be addressed (e.g., lack of fault data).

Accordingly, to contribute towards this unexplored field, an analysis of a total of seven time series imaging approaches is performed. The presentation of this analysis stems from the potential that these approaches have demonstrated in analogous sectors, such as in the energy sector. The seven time series imaging approaches refer to: 1) GASF, 2) GADF, 3) MTF, 4) MTM, 5) RP, 6) compound of GASF-

GADF-MTF, and 7) compound of GASF-GADF-MTF-MTM-RP. The CNN model is considered as the image classifier.

The compound of GASF-GADF-MTF-MTM-RP outperformed the remaining approaches, which achieved the maximum accuracy that can be obtained in any classification task. Such a fact demonstrates the undeniable potential of both time series imaging approaches and image classifiers, and thus further research in this field is required. The analysis of further time series imaging approaches and image classifiers is just an example of the future work that the authors are considering in their upcoming research agenda.

References

Cai, C. Weng, X. Zhang, C. (2017). A novel approach for marine diesel engine fault diagnosis. Cluster Computing 20, pp. 1691-1702, doi: https://doi.org/10.1007/s10586-017-0748-0.

Department for Transport. (2019). Technology and Innovation in UK Maritime: The case of Autonomy, pp. 1-60.

Eckmann, J.-P. Oliffson Kamphorst, S. Ruelle, D. (1987). Recurrence Plots of Dynamical Systems. Europhysics Letters.

Fahim, S. R. Sarker, S. K. Muyeen, S. M. Sheikh, M. R. I. Das, S. K. Simoes, M. (2021a). A Robust Self-Attentive Capsule Network for Fault Diagnosis of Series-Compensated Transmission Line. IEEE Transactions on Power Delivery 36, pp. 3846-3857, doi: https://doi.org/10.1109/TPWRD.2021.3049861.

Fahim, S. R. Muyeen, S. M. Sarker, Y. Sarker, S. K. Das, S. K. (2021b). An Agreement Based Dynamic Routing Method for Fault Diagnosis in Power Network with Enhanced Noise Immunity. 2021 31st Australasian Universities Power Engineering Conference, pp. 1-5 doi: https://doi.org/10.1109/AUPEC52110.2021.9597762.

Fahim, S. R. Sarker, Y. Sarker, S. K. Sheikh, M. R. I. Das, S. K. (2020a). Self-attention convolutional neural network with time series imaging based feature extraction for transmission line fault detection and classification. Electric Power Systems Research 187, pp. 1-12, doi: https://doi.org/10.1016/j.epsr.2020.106437.

Fahim, S. R. Islam Sarker, M. R. Arifuzzaman, M. Hosen, M. S. Sarker, S. K. Das, S. K. (2020b). A novel Approach to Fault Diagnosis of High Voltage Transmission line – A Self Attentive Convolutional Neural Network Model. 2020 IEEE Region 10 Symposium, pp. 1329-1332, doi: https://doi.org/10.1109/TENSYMP50017.2020.9230660.

Grandini, M. Bagli, E. Visani, G. (2020). Metrics for Multi-Class Classification: An Overview. Computer Science. ArXiv, pp. 1-17, URL: https://arxiv.org/pdf/2008.05756.pdf.

Han, P. Ellefsen, A. L. Li, G. Æsøy, V. Zhang, H. (2021). Fault Prognostics Using LSTM Networks: Application to Marine Diesel Engine. IEEE Sensors Journal, pp. 1-8, doi: https://doi.org/10.1109/JSEN.2021.3119151.

Hou, L. Zhang, J. Du, B. (2020). A Fault Diagnosis Model of Marine Diesel Engine Fuel Oil Supply System Using PCA and Optimized SVM. Journal of Physics: Conference Series 1576, pp. 1-9, doi: https://doi.org/10.1088/1742-6596/1576/1/012045.

Li, Y. Huang, X. Ding, P. Zhao, C. (2021). Wiener-based remaining useful life prediction of rolling bearings using improved Kalman filtering and adaptive modification. Measurement 182, pp. 1-17, doi: https://doi.org/10.1016/j.measurement.2021.109706.

Lloyd's List. (2021). Outlook 2021. Shipping accelerates towards an uncertain future, pp. 1-66.

London Economics, NLA International, Marine South East. (2021). Consultancy Research into the UK Maritime Technology Sector, pp. 1-151.

Marine Accident Recommendations and Statistics (MAIB). (2020). Annual report, pp. 1-79.

Senemmar, S. Zhang, J. (2021). Deep Learning-based Fault Detection, Classification, and Locating in Shipboard and Power Systems. 2021 IEEE Electric Ship Technologies Symposium, pp. 1-6, doi: http://doi.org/10.1109/ESTS49166.2021.9512342.

Tan, Y. Zhang, J. Tian, H. Jiang, D. Guo, L. Wang, G. Lin, Y. (2021). Multi-label classification for simultaneous fault diagnosis of marine machinery: A comparative study. Ocean Engineering 239, pp. 1-11, doi: https://doi.org/10.1016/j.oceaneng.2021.109723.

Tan, Y. Tian, H. Jiang, R. Lin, Y. Zhang, J. (2020). A comparative investigation of data-driven approaches based on one-class classifiers for condition monitoring of marine machinery system. Ocean Engineering 201, pp. 1-12, doi: https://doi.org/10.1016/j.oceaneng.2020.107174.

Thetius-Inmarsat. (2021). A changed world. The state of digital transformation in a post COVID-19 maritime industry, pp. 1-52.

Velasco-Gallego, C. Lazakis, I. (2020). Real-time data-driven missing data imputation for short-term sensor data of marine systems. A comparative study. Ocean Engineering 218, pp. 1-23, doi: https://doi.org/10.1016/j.oceaneng.2020.108261.

Velasco-Gallego, C. Lazakis, I. (2021). A novel framework for imputing large gaps of missing values from time series sensor data of marine machinery systems. Ships and Offshore Structures, pp. 1-11, doi: https://doi.org/10.1080/17445302.2021.1943850.

Velasco-Gallego, C. Lazakis, I. (2022). A real-time data-driven framework for the identification of steady states of marine machinery. Applied Ocean Research 121, pp. 1-12, doi: https://doi.org/10.1016/j.apor.2022.103052.

Wang, Z. Oates, T. (2015). Encoding Time Series as Images for Visual Inspection and Classification Using Tiled Convolutional Neural Networks. AAAI Workshop, pp. 1-7.

Wang, S. Wang, J. Wang, R. (2020). A novel scheme for intelligent fault diagnosis of marine diesel engine using the multi-information fusion technology. IOP Conference Series Materials Science and Engineering 782, pp. 1-12, doi: https://doi.org/10.1088/1757-899X/782/3/032022.

Yao, Y. Wang, J. Xie, M. Hu, L. Wang, J. (2020). A new approach for fault diagnosis with full-scope simulator based on state information imaging in nuclear power plant. Annals of Nuclear Energy 141, pp. 1-9, doi: https://doi.org/10.1016/j.anucene.2019.107274.

Zhao, Z. Cerf, S. Birke, R. Robu, G. Bouchenak, S. Mokhtar, S. B. Chen, L. Y. (2019). Robust Anomaly Detection on Unreliable Data. 49th Annual IEEE/IFIP International Conference on Dependable Systems and Networks (DSN), pp. 630-637, doi: https://doi.org/10.1109/DSN.2019.00068.

Zio, E. (2022). Prognostics and Health Management (PHM): Where are we and where do we (need to) go in theory and practice. Reliability Engineering and System Safety 218, pp. 1-16, doi: https://doi.org/10.1016/j.ress.2021.108119.